1/3 magnetization plateau and frustrated ferrimagnetism in a sodium iron phosphite

A.N. Vasiliev,[1,2,3] O.S. Volkova,[1,2,3] E.A. Ovchenkov,[1] E.A. Zvereva,[1] I. Munaò,[4] L. Clark,[4] P. Lightfoot,[4] E.L. Vavilova,[5,6] S. Kamusella,[6] H.-H. Klauss,[6] J. Werner,[7] C. Koo,[7] R. Klingeler,[7] and A.A. Tsirlin[8]

[1]Physics Faculty, Lomonosov Moscow State University, 119991 Moscow, Russia
[2]National University of Science and Technology "MISiS", 119049 Moscow, Russia
[3]Institute of Physics and Technology, Ural Federal University, 620002 Ekaterinburg, Russia
[4]School of Chemistry, University of St Andrews, Fife KY16 9ST, UK
[5]Zavoisky Institute of Physics and Technology, RAS, Kazan 420029, Russia
[6]Institute of Solid State Physics, Dresden Technical University, D-01069 Dresden, Germany
[7]Kirchhoff Institute of Physics, Heidelberg University, D-69120 Heidelberg, Germany
[8]Experimental Physics VI, Center for Electronic Correlations and Magnetism, Institute of Physics, University of Augsburg, D-86135 Augsburg, Germany

Mössbauer spectroscopy of $NaFe_3(HPO_3)_2(H_2PO_3)_6$

The temperature dependence of the isomer shift $\delta(T)$ (Fig. S1), which is shared by both sextets, is described without anomalies by an ordinary Debye model, yielding a Debye temperature Θ_D = 461(5) K, which was used for specific heat analysis. This value is not reproduced by the temperature dependence of the spectrum area (represented by effective thickness t_a Fig. S1 inset), which has most likely experimental reasons, i.e. a change of the non-resonant underground due to the thermal expansion of the sample rod.

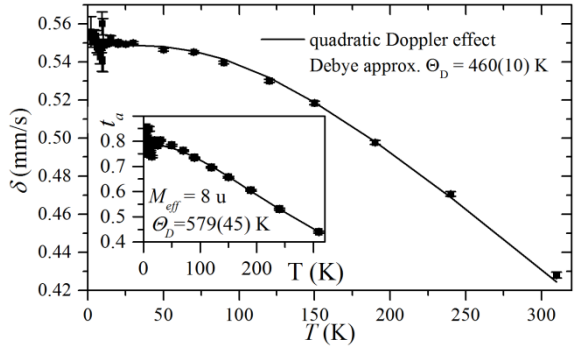

Figure S1. The temperature dependence of isomer shift δ

The observed quadrupole interaction of about 0.17 mm/s for temperatures between 300 K and 10 K correspond to a principal component of the electric field gradient (EFG) V_{zz} on the order of -10 V/Å^2, assuming an axial symmetry of the EFG. This symmetry naturally arises from the weakly distorted FeO_6 octahedra. Given the large Sternheimer antishielding factor of about –10 in $^{57}Fe^{3+}$ [1], the measured EFG can be fully explained by the lattice contribution due to a small distortion of 0.02 Å as mentioned before, neglecting valence orbital contribution due to the high spin valence. Considering the EFG arising from the lattice only, the temperature dependence $V_{zz}(T)$ indeed can be fitted with a Debye model describing thermal expansion using the Debye temperature Θ_D = 460 K, as shown in Fig. S2. For $T < T_C$ we set Vzz =-11.4 V/Å^2 to extract the polar angle θ = 62(1)° between the principal axis of the EFG and the internal magnetic field on the Fe nuclei.

We applied an external field transverse to the gamma beam to study the local susceptibility of the magnetic moments at 5 K (Fig. S3). The ^{57}Fe nuclear probe is sensitive to

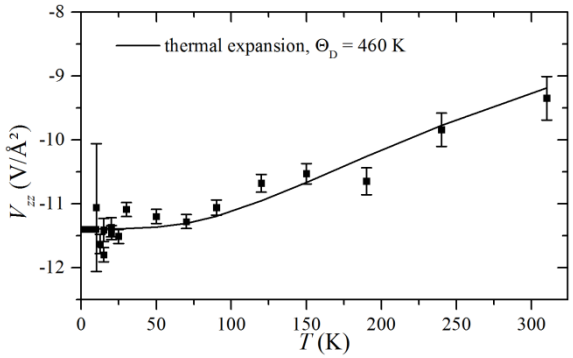

Figure S2. The temperature dependence of the principal component V_{zz} of the EFG

the following quantities: (a) the absolute value of the total field B_{tot}, (b) the effective angle β_{eff} between the total field and the gamma beam and (c) the width of the field distribution arising from different angular superposition of internal moments and applied field.

(a) The absolute value $\boldsymbol{B_{tot}} = \boldsymbol{B_{ex}} + \boldsymbol{B_{hyp}}$ depends on the orientation and the strength of the magnetic hyperfine field $\boldsymbol{B_{hyp}}$ and will represent itself in the amount of splitting of the sextet. For moderate temperature of $0.5 < T/Tc < 1$ an applied field might always be able to increase the ordered electronic moment and thus B_{hyp} as seen by the nucleus. For sufficient high B_{hyp} values this might even overcompensate the typical effects observed for a ferro- (FM) and antiferromagnetically (AFM) coupled moments: for a FM moment the total field will be reduced by the external field as soon as the moments get aligned parallel to the field. This cancellation is due to the negative coupling constant of the moment to the nucleus via the Fermi contact interaction in ^{57}Fe. Likewise an antiferromagnetically coupled moment (antiparallel to the applied field) will show an increasing total field.
(b) In the transverse applied field geometry the effective angle β_{eff} is related to the angle α between field and moment by $\cos^2\beta_{eff} = \langle \sin^2 \alpha \rangle / 2(b^2+1-2b\cos\alpha)\rangle$, where the averaging is in real space and $b=B_{ex}/B_{hyp}$. β_{eff} influences the intensity of the 2nd and 5th line. In the transverse geometry there are two specific angles, namely the magic angle $\beta_{eff} = 54.7°$ representing a random orientation of the moments and thus an ordinary powder-sextet (3:2:1:1:2:3 intensities) and $\beta_{eff} = 90°$ where all moments are aligned to the magnetic field (3:4:1:1:4:3 intensities).
(c) An antiferromagnetic coupling or an anisotropy field B_J prevent the magnetic moments to immediately align to the field. In terms of Mössbauer spectroscopy, both effects are hardly distinguishable in polycrystalline samples. Because of the random orientation of anisotropy axis and thus the slightly pinned moments the vector sum of internal and external values yields different absolute values. Because Mössbauer spectroscopy is a local probe the measured ensemble will show a broad distribution of field values, resulting in a line broadening, which is maximal at $B_{ex}/B_A \approx 0.35$ in powder samples.

Interestingly both sextets show a large line broadening around 1 T indicating a large field distribution due to anisotropy field. Subsequently the lines get narrow again and β_{eff} noticeably tends to 90° already at 2 T applied field (Fig. S4). Both effects can be typically described by a uniaxial anisotropic magnetism with a negative anisotropy field, i.e. an easy plane anisotropy of B_A=-3 T. β_{eff} approaches arccos(1/sqrt(6)) ≈ 66° for B_{ex} close to zero in powder, which is in agreement with our data and specific for the easy plane case. Nevertheless it should be noted, that this moderate easy plane anisotropy is in stark contrast to the weak easy axis as suggested by EPR spectroscopy. Furthermore both sextets show an increasing splitting upon application of the external fields. The total field increases faster than a simple constructive summation of the internal and the applied field could account for. The commonly applied static Hamiltonian

$$H \sim -B_J \cos(\theta_1-\theta_2) - B_A\,(\cos(\theta_1-\zeta) + \cos(\theta_2-\zeta)) - B_{ex}\,(\cos(\theta_1) + \cos(\theta_2)),$$

which was assumed so far, seems inapplicable for T/T_c=0.5. In this context β_{eff} is to be seen as an expectation value rather than an average value. Due to the non-static character we limited our final analysis to the phenomenological formula used in the main text.

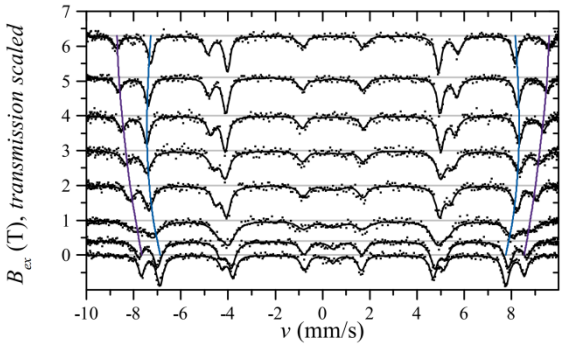

Figure S3. Transverse field Mössbauer spectra

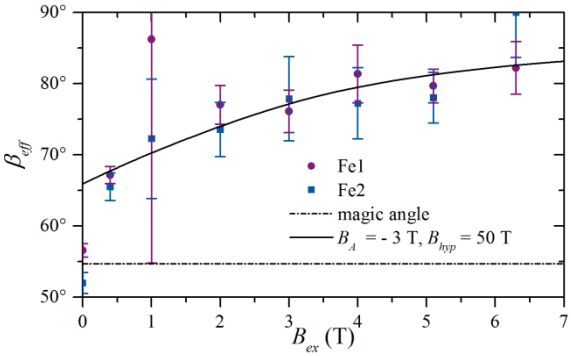

Figure S4. Temperature dependence of the effective angle β_{eff} between gamma beam and total field.

From the magnetic texture point of view, i.e. β_{eff}, the moments are predominantly aligned for B_{ex} = 2 T. However for Fe2 the total field is still increasing, but the trend continuously reverses and finally approaches a linear decrease representing a ferromagnetic alignment of the spins. For Fe1 a reduction of the gradient can be observed, but no reverse.

We give the following explanation of the data: first the anisotropy field is quenched and the moments get aligned like a ferrimagnet, i.e. sublattice Fe2 parallel and Fe1 antiparallel to the applied field. Subsequently the magnetic hyperfine field is enhanced by the applied field (corresponds to the slightly inclined 1/3-plateau in magnetization data), because the compound is at finite temperature $T/T_c \approx 0.5$. Last, AFM coupling of Fe1 to Fe2 will be quenched and all moments become aligned parallel to the applied field.

For Fe1 the additional breaking of the exchange coupling to the Fe2 dimers considerably influences the physical behavior, especially for $B_{ex} > 5$ T when the braking of the coupling takes place. At 6.3 T the Fe2 moments are perfectly aligned (β_{eff} = 90°), while this is not the case for Fe1. Unfortunately higher fields where not available, but a temporary decrease of β_{eff} for the Fe1 site is expected for B_{ex}=B_c.

The model parameter $B_s \approx 52$ T for Fe1 used in the phenomenological model in the main text is lower than B_{hyp}(2 K) indicating, that the competition of B_{ex} and B_J is already important at lower fields.

1. Y.L. Chen and D.P. Yang, Mössbauer effect in lattice dynamics: experimental techniques and applications, John Wiley & Sons, 2007.

Table S1. Relaxed hydrogen positions in the $NaFe_3(HPO_3)_2(H_2PO_3)_6$ structure [14]. Experimental lattice parameters a = 7.5302 Å, b = 9.1696 Å, c = 9.4732 Å, α = 118.063°, β = 101.274°, γ = 101.192°, and the triclinic space group $P\bar{1}$ were used. The last column shows the P and O atoms that the hydrogens are linked to.

	x/*a*	*y*/*b*	*z*/*c*	
H1	0.92517	0.35044	0.95535	P3
H2	0.63676	0.46346	0.44432	P4
H3	0.55411	0.83333	0.92131	P2
H4	0.99043	0.75964	0.32566	P1
H5	0.77954	0.94086	0.30216	O9
H6	0.43336	0.43748	0.73360	O11
H7	0.74926	0.96581	0.76451	O12